Male minipuberty involves the gonad-independent activation of preoptic nNOS neurons

Virginia Delli, Julien Dehame, Delphine Franssen, S. Rasika, Anne-Simone Parent, Vincent Prevot, Konstantina Chachlaki

Invited Review Article is part of Special Issue Nitric oxide signaling from Synapse to Disease
Guest Editors Joern Steinert & Haitham Amal

Male minipuberty involves the gonad-independent activation of preoptic nNOS neurons

Virginia Delli [1,2], Julien Dehame [1,2], Delphine Franssen [3], S Rasika [1,2], Anne-Simone Parent [3,4], Vincent Prevot [1,2], Konstantina Chachlaki [1,2,5 ©],

[1] Univ. Lille, CHU Lille, Inserm, Laboratory of Development and Plasticity of the Neuroendocrine Brain, Lille Neuroscience and Cognition, UMR-S 1172, F-59000 Lille, France
[2] FHU 1,000 days for Health, School of Medicine, F-59000 Lille, France
[3] GIGA Neurosciences, Neuroendocrinology Unit, University of Liège, Liège, Belgium
[4] Department of Pediatrics, University Hospital Liège, Liège, Belgium
[5] University Research Institute of Child Health and Precision Medicine, National and Kapodistrian University of Athens, "Aghia Sophia" Children's Hospital, Athens, Greece

[©] *Corresponding author*: Konstantina Chachlaki (Konstantina.Chachlaki@inserm.fr; +33 761-43-45-79)

Abstract

Background. The maturation of the hypothalamic-pituitary-gonadal (HPG) axis is crucial for the establishment of reproductive function. In female mice, neuronal nitric oxide synthase (nNOS) activity appears to be key for the first postnatal activation of the neural network promoting the release of gonadotropin-releasing hormone (GnRH), i.e. minipuberty. However, in males, the profile of minipuberty as well as the role of nNOS-expressing neurons remain unexplored.

Methods. nNOS-deficient and wild-type mice were studied during postnatal development. The expression of androgen (AR) and estrogen receptor alpha (ERα) as well as nNOS phosphorylation were evaluated by immunohistochemistry in nNOS neurons in the median preoptic nucleus (MePO), where most GnRH neuronal cell bodies reside, and the hormonal profile of nNOS-deficient male mice was assessed using previously established radioimmunoassay and ELISA methods. Gonadectomy and pharmacological manipulation of ERα were used to elucidate the mechanism of minipubertal nNOS activation and the maturation of the HPG axis.

Results. In male mice, minipubertal FSH release occurred at P23, preceding the LH surge at P30, when balanopreputial separation occurs. Progesterone and testosterone remained low during minipuberty, increasing around puberty, whereas estrogen levels were high throughout postnatal development. nNOS neurons showed a sharp increase in Ser^{1412} phosphorylation of nNOS at P23, a phenomenon that occurred even in the absence of the gonads. In male mice, nNOS neurons did not appear to express AR, but abundantly expressed ERα throughout postnatal development. Selective

pharmacological blockade of ERα during the infantile period blunted Ser^{1412} phosphorylation of nNOS at P23.

Conclusions. Our results show that the timing of minipuberty differs in male mice when compared to females, but as in the latter, nNOS activity in the preoptic region plays a role in this process. Additionally, akin to male non-human primates, the profile of minipuberty in male mice is shaped by sex-independent mechanisms, and possibly involves extragonadal estrogen sources.

Keywords: minipuberty; neuronal nitric oxide synthase (nNOS); gonadotropin-releasing hormone (GnRH); estrogen; hypothalamus

Introduction

Reproduction is orchestrated by the hypothalamus, and specifically neurons located in the median preoptic nucleus (MePO) that synthesize gonadotropin-releasing hormone (GnRH) and release it at their nerve terminals in the median eminence of the hypothalamus (Herbison, 2015; Prevot, 2015; Moenter, 2017). From there, GnRH is carried by the pituitary portal circulation to the anterior pituitary, where it stimulates the synthesis and secretion of the gonadotropins, luteinizing hormone (LH) and follicle-stimulating hormone (FSH). The gonadotropins, as indicated by their name, act on the gonads (i.e., the testes and ovaries) to control the production of sperm and eggs and the secretion of sex steroids. The disruption in any of the above steps of the hypothalamic-pituitary-gonadal (HPG) axis can have a detrimental impact on fertility. However, to elicit gonadotropin release, coordinated GnRH neuronal activity that can promote meaningful episodes of GnRH secretion is required. This neuronal activity is controlled by a dynamic array of internal and external signals involving various neuropeptides, hormones and neurotransmitters, including gonadal steroids themselves as well as the gaseous second messenger nitric oxide (NO) (Chachlaki et al., 2017a; Chachlaki and Prevot, 2020; Delli et al., 2021).

The first postnatal activation of the HPG axis, which occurs during the infantile period in both humans and mice, is attested to by a substantial release of FSH and LH (Kuiri-Hänninen et al., 2014; Prevot, 2015). Neuronal NO synthase (nNOS) neurons, which produce NO, are morphologically and functionally associated with GnRH neuronal cell bodies and dendrites in the MePO and the organum vasculosum of the lamina terminalis (OVLT or OV) (Chachlaki et al., 2017b). As such, they are ideally positioned to play a role in the rapid integration and transmission of both gonadal and metabolic signals to GnRH neurons, including during minipuberty. Increased nNOS activity – and hence NO release – during minipuberty, by modulating the transcription, activity and release of GnRH (Messina et al., 2016), could thus control the secretion of gonadotropins and subsequently, the maturation and function of the neuroendocrine axis (Chachlaki et al., 2022).

In humans, gonadotropin profiles during minipuberty are sexually dimorphic. Minipuberty induces an increase in the level of estradiol, promoting the maturation of ovarian follicles in girls, whereas in boys, urinary levels of FSH are positively correlated with testicular growth, increasing the level of circulating testosterone. The impairment of minipuberty may hence impede the development of the reproductive system, affecting puberty and subsequently, adult fertility (Kuiri-Hänninen et al., 2014). Interestingly, female nNOS-deficient mice demonstrate exacerbated minipuberty, with aberrantly high FSH and LH levels during infantile life (Chachlaki et al., 2022), and estrogen plays a crucial role in the minipubertal activation of nNOS neurons and the subsequent maturation of the HPG axis (Chachlaki et al., 2017b; Chachlaki et al., 2022). However, not much is known about the mechanisms at work during minipuberty in males.

Here, we explored whether the regulation of minipuberty was sex-dependent, and attempted to determine the role played by NO signaling in the control of male minipuberty.

Materials and Methods

ANIMALS

All C57Bl/6J mice were housed under specific pathogen-free conditions in a temperature-controlled room (21-22°C) with a 12h light/dark cycle and ad libitum access to food and water. Experiments were performed on male and female C57BL/6J mice (Charles River Laboratories), Nos1-deficient (Nos1-/-, B6.129S4-Nos1tm1Plh/J) mice (26) and Gnrh::Gfp mice (a generous gift of Dr. Daniel J. Spergel, Section of Endocrinology, Department of Medicine, University of Chicago, IL) (97). Nos1-/-; Gnrh::Gfp mice were generated in our animal facility by crossing Nos1-/+ mice with Gnrh::Gfp mice. Animal studies were approved by the Institutional Ethics Committees for the Care and Use of Experimental Animals of the Universities of Lille; all experiments were performed in accordance with the guidelines for animal use specified by the European Union Council Directive of September 22, 2010 (2010/63/EU) and were approved by the French Department of Research (APAFIS#2617-2015110517317420v5).

ORCHIDECTOMY

Two independent litters of Gnrh::Gfp mice were used for orchidectomies. At postnatal day 10 (P10) male littermates were either orchiectomized (ORX), or just laparotomized (Sham), under general anaesthesia (induction 4% in air 2 L/min, then 1.5% in air 0.3 L/min), after local injection of lidocaine (30 microliters of a 0.5% solution, s.c.) and preemptive Meloxicam treatment (5 mg/kg).

MPP TREATMENT

Gnrh::Gfp pups from three independent litters received a daily intraperitoneal injection of MPP dihydrochloride (1,3-Bis(4-hydroxyphenyl)-4-methyl-5-[4-(2-piperidinylethoxy)phenol]-1H-

pyrazole dihydrochloride hydrate, Methyl-piperidino-pyrazole hydrate; 0.1mg/kg; dissolved at 10mM in DMSO/ saline mixture), a high selective antagonist of estrogen receptor α (Tocris, Cat# 1991,), or vehicle (DMSO/ saline). Treatment started at postnatal day 10 and terminated at postnatal day 23 (lights on). Upon completion of the treatment blood was collected (lights off) and mice were perfused and processed for IHC analysis of brain sections.

QUANTITATIVE RT-PCR ANALYSES

For transcriptomic analysis all animals used were sacrificed by decapitation at the postnatal day indicated. The preoptic area of the hypothalamus (POA), the pituitary gland and the testis were collected in an Eppendorf tube and snap frozen in liquid nitrogen (or post-fixed for histological analysis, see below). The POA and the pituitary gland were dissociated in 40µl of extraction buffer [0.1% Triton® X-100 (Sigma-Aldrich) and 0.4 U/µl RNaseOUT™ (Life Technologies Invitrogen, Cat# 10777019)] and the testicle was processed for RNA extraction using the E.Z.N.A.® Total RNA Kit II (Omega Bio-Tek, Cat# R6934-02, Lot# R693425535-3,), following the manufacturers' protocol. The samples were reverse transcribed using Transcriptase inverse MultiScribe™ (Invitrogen, Cat# 4311235, Lot# 01105639). Real-time PCR was carried out on Applied Biosystems 7900HT Fast Real-Time PCR System using exon-boundary-specific TaqMan® Gene Expression Assays (Applied Biosystems): Anti-Mullerian hormone (*Amh*-Mm00431795_g1), Androgen receptor (*Ar*-Mm00442688_m1), Cytochrome P450, family 19, subfamily a, polypeptide 1 (*Cyp19a1*-Mm00484049_m1), Cytochrome P450, family 17, subfamily a, polypeptide 1 (*Cyp17a1*-Mm00484040_m1), Estrogen receptor1 (alpha) (*Ers1*-Mm00433149_m1), Estrogen receptor 2 (beta) (*Esr2*-Mm00599821_m1), Follicle stimulating hormone beta (*Fshb*-Mm00433361_m1), Follicle stimulating hormone receptor (*Fshr*-Mm00442819_m1), Gonadotropin releasing hormone 1 (*Gnrh1*-Mm01315605_m1), Gonadotropin releasing hormone receptor (*Gnrhr*-Mm00439143_m1), Hydroxysteroid (17-beta) dehydrogenase 3 (*Hsd17b3*-Mm00515131_m1), 3 beta- and steroid delta-isomerase 6 (*Hsd3b6*-Mm07306505_m1), Inhibin alpha (*Inha*-Mm00439683_m1), Inhibin beta (*Inhbb*- Mm03023992_m1), Insulin-like 3 (*Insl3*-Mm01340353_m1), Kiss-1 metastasis-suppressor (Mm03058560_m1), Kiss1 receptor (*Kiss1r*-Mm00475046_m1), Luteinizing hormone beta (*Lhb*-Mm00656868_g1), Luteinizing hormone receptor (*Lhcgr*-Mm00442931_m1), Nitric oxide synthase 1, neuronal (*Nos1*- Mm01208059_m1), Progesterone receptor (*Pgr*-Mm00435628_m1). Control housekeeping genes: Eukaryotic 18S rRNA (*Rn18S*-Mm03928990_g1), Actin beta (*Actb*-Mm00607939_s1).

ANALYSIS OF MALE GONADS

After surgical removal, testis was dried on filter paper and weighted. Testicular weight was eventually normalized over total body weight of the animal prior to sacrifice. For histological

preparations, testis was fixed in 4% PFA overnight. Tissue was then progressively dehydrated with ethanol/xylene baths, before being paraffin-embedded. Testis were cut in 6µm sections with a microtome (Leica, RM2245) and stained with hematoxylin and eosin. Sections were eventually digitalized using Zeiss Axioscan Z1 with a 20×/0.8 objective in brightfield. For each animal, the number of seminiferi tubules and the cross-section area were manually counted using ZEN (ZEISS). The quantification was realized in the whole testis every 50µm, excluding the extremities of the organ (150 µm).

IMMUNOHISTOCHEMISTRY

Tissue Preparation: Mice were anesthetized with a lethal dose of pentobarbital (DOLÉTHAL®, 5mg/kg) and locally treated with Lidocain (30 µl of a 0.5% solution). Animals were perfused thoroughly with cold saline, until exsanguination, then perfused with cold fixative solution [4% paraformaldehyde (PFA), in 0.1M PB, pH 7.4]. The brain was extracted and post-fixed with the same fixative solution for 2h at 4°C, then cryoprotected in PB 0.1M 20% sucrose for 24h at 4°C. Afterwards, the brain was embedded in OCT medium (Tissue-Tek), frozen on dry ice, and stored at −80°C until sectioning. Tissues were cryosectioned (Leica cryostat) coronally at 35 µm (free-floating sections).

Antibodies: The goat polyclonal anti-nNOS antibody (1:1000; Cat# OSN00004G, Lot#VF3001511) and the rabbit polyclonal anti-Ser1412 phospho-nNOS antibody (1:500; Cat# PA1-032, Lot# UB274796) were purchased from ThermoScientific. The rat polyclonal anti-GnRH (1:2500; Cat# EH1044) was a generous gift from Professor Hrabovszky (Laboratory of Reproductive Neurobiology, Institute of Experimental Medicine, Budapest, Hungary). The rabbit polyclonal anti-estrogen receptor α (1:500; Cat# 06–935, Lot#3701815) and anti-androgen receptor (1:1000; Cat# 06-680, Lot# 38113557) were purchased from Millipore. The Alexa Fluor 647-conjugated donkey anti-goat secondary antibody (1:500; Cat# A21447, Lot# 2465096) used for nNOS immunolabeling, the Alexa Fluor 568-conjugated donkey anti-rabbit secondary antibody (1:500; Cat# A10042, Lot# 2306809) used for phospho-nNOS, androgen receptor and estrogen receptor α immunolabeling, and the Alexa Fluor 488-conjugated donkey anti-rat secondary antibody (1:500; Cat# A21208, Lot# 2180272) used for GnRH immunolabeling, were purchased from Invitrogen.

Immunolabeling: Sections were washed 3 times for 5 minutes each in PB 0.1M and then incubated in blocking solution (5% NDS, 0.3% Triton X-100 in PB 0.1M) for 1 hour at room temperature. Sections were incubated for 48-72 hours at 4°C with the primary antibodies diluted in blocking solution, then rinsed 3 times for 5 minutes each in PB 0.1M. The sections were incubated with secondary antibodies diluted in PB 0.1M for 1h at room temperature, then rinsed in PB 0.1M 3 times for 5 minutes each, and finally incubated 7 minutes with DAPI (1:5000 in PB 0.1 M) for nuclear staining. After washing, sections were mounted on glass slides and coverslipped under Mowiol medium.

Digital image acquisition: Images were acquired with a Zeiss Axio Imager Z2 microscope (Zeiss, Germany). Alexa 488 was imaged using a 495 nm beam splitter with an excitation wavelength set at 450/490 nm and an emission wavelength set at 500/550 nm. Alexa 568 was imaged using a 570 nm beam splitter with an excitation wavelength set at 538/562 nm and an emission wavelength set at 570/640 nm. Alexa 647 was imaged by using a 660 nm beam splitter with an excitation wavelength set at 625/655 nm and an emission wavelength set at 665/715 nm. Nuclear staining (Hoechst) was imaged by using a 395 nm beam splitter with an excitation wavelength set at 335/383 nm and an emission wavelength set at 420/470 nm. Images were acquired with a Plan-Apochromat 20X objective (numerical aperture NA = 0.80; thread type M27). Z-stack images were taken every 1 µm, for a total of 20 µm per sections. All the images are presented as maximal intensity projections (MIP) of three-dimensional volumes along the optical axis. Images to be used for figures were adjusted for brightness and contrast using Photoshop (Adobe Systems, San Jose, CA).

Cell counting: The nomenclature of brain regions used in this article corresponds to that described in the Allen brain atlas (Lein et al., 2007). The quantification of nNOS neurons co-expressing estrogen receptor α or androgen receptor was undertaken by counting the number of single-labeled nNOS-positive neurons and double-labeled nNOS/estrogen receptor-α or nNOS/androgen receptor cells in the OV, represented by plate 49 of the Allen Developing Mouse Brain Atlas. Cell counts were carried out unilaterally, represented as percentage of nNOS neurons co-expressing estrogen receptor α or androgen receptor, and the values from each mouse were averaged to determine mean counts and SEM for each age group.

MEASUREMENT OF CIRCULATING HORMONES

Radioimmunoassay (FSH): Serum FSH measurement was carried out using a double antibody method and the rat-FSH RIA kit supplied by the National Institutes of Health (Dr. A. F. Parlow, NIDDK-NHPP, Torrance, CA). The primary antibody (NIDDK anti– rFSH-S-11, AB_2687903) was used at a dilution factor of 1/31,250. Rat FSH antigen (NIDDK rFSH-I, AFP-5178B) was labeled with 125I by the chloramine-T method. The hormone concentration was calculated using the rat FSH reference preparation (NIDDK rFSH-RP-2, AFP-4621B) as standard. The intra-assay and inter-assay coefficients of variation were 7 % and 10 %. The sensitivity of the assay was 0.03 ng/100 µl. FSH levels were measured using radioimmunoassay as previously described (Messina et al., 2016).

Elisas (LH, 17β-estradiol, Inhibin B, AMH, Testosterone, Progesterone): Plasma LH was measured using a highly sensitive Enzyme-linked Immunosorbent Assay (ELISA) as described elsewhere (Steyn et al., 2013). The accuracy of hormone measurements was confirmed by the assessment of rodent serum samples of known concentration (external controls). Serum 17β-estradiol concentration was determined by ELISA (Demeditec Diagnostics, Cat# DE2693) as described previously (Fonseca et al., 2012). Inhibin B was measured using a commercial Enzyme-linked Immunosorbent Assay (ELISA) multispecies kit (AnshLabs, Cat# AL-163), following the manufacturers' protocol. AMH

was measured using the commercial rat and mouse AMH Enzyme-linked Immunosorbent Assay (ELISA) kit (AnshLabs, Cat# AL-113) as described elsewhere (Devillers et al., 2019). Plasmatic concentrations of progesterone were assessed using a commercial kit (Demeditec Diagnostics, Cat# DEV9988), following the manufacturers' protocol. Testosterone was measured using the commercial rat/mouse ELISA kit (Demeditec Diagnostics, Cat# DEV9911).

STATISTICAL ANALYSIS

All analyses were performed using Prism 7 (Graphpad Software, San Diego, CA) and assessed for normality (Shapiro–Wilk test) and variance, when appropriate. Sample sizes were chosen according to standard practice in the field. The investigators were blinded to the group allocation during the experiments. For each experiment, replicates are described in the figure legends. For animal studies, data were compared using an unpaired two-tailed Student's t-test or a one-way ANOVA for multiple comparisons against the control condition followed by Dunnett multiple comparison post-hoc test. Data not following normal distribution were analyzed using either a Mann-Whitney U test (comparison between two experimental groups) or Wilcoxon/Kruskal-Wallis test (comparison between three or more experimental groups) followed by a Dunn's post hoc analysis. The number of biologically independent experiments, sample size, P values, age and sex of the animals are all indicated in the main text or figure legends. All experimental data are indicated as mean ± s.e.m. The significance level was set at $P < 0.05$. Symbols in figures correspond to the following significance levels: ns. $P > 0.05$, * $P < 0.05$, ** $P < 0.001$, ***$P < 0.0001$.

Results

Minipubertal GnRH axis maturation differs in male and female mice

In female mice, FSH and LH levels peak at around postnatal day (P) 12, returning to basal levels after weaning, at around P23 (Prevot et al., 2003; François et al., 2017; Chachlaki et al., 2022). In order to assess the timing of minipuberty in male mice, we analyzed gonadotropin levels, i.e. FSH and LH, during different developmental stages: infantile (P12), juvenile (P23, P30) and peripubertal (P50). Interestingly, in male mice, circulating FSH levels, reflecting *Gnrh* mRNA levels in the POA, peaked at P23, i.e. at a time when minipuberty in females has terminated (Chachlaki et al., 2022), returning to baseline by P30 (Fig. 1a, Suppl. Fig. 4). This minipubertal increase in *GnRH* production does not seem to involve the kisspeptin pathway, since both kiss1 and kiss1r mRNA levels remained unchanged during this period (Suppl. Fig. 4). Surprisingly, however, serum LH levels in male mice remained very low throughout the infantile and early juvenile period, but increased at P30, a week later than FSH and around the time that balanopreputial separation normally occurs, returning to basal values at P50 (Fig. 1b). Minipuberty thus seems to be a biphasic period rather than a single time point or event in males.

To better understand the interplay between the maturational processes taking place both in the hypothalamus and along the HPG axis of male mice, we measured circulating levels of the sex steroid hormones (estradiol, progesterone and testosterone) as well as inhibin B and AMH during postnatal development. Circulating testosterone levels in male mice remained low until the juvenile stage, abruptly increased peripubertally (P50) (Fig. 1e). In contrast, serum progesterone levels steadily increased over the period studied (Fig. 1f), while serum estradiol levels were consistently elevated during postnatal development, with no marked difference between the various stages studied (Fig. 1g). Circulating AMH levels revealed relatively high levels in the serum of P12 male mice, but dropped by almost 95% by the time minipuberty began at P23 (Fig. 1d). Similarly, inhibin B levels decreased by more than half between P12 and P23, when FSH levels peaked in male wild-type mice (Fig. 1c).

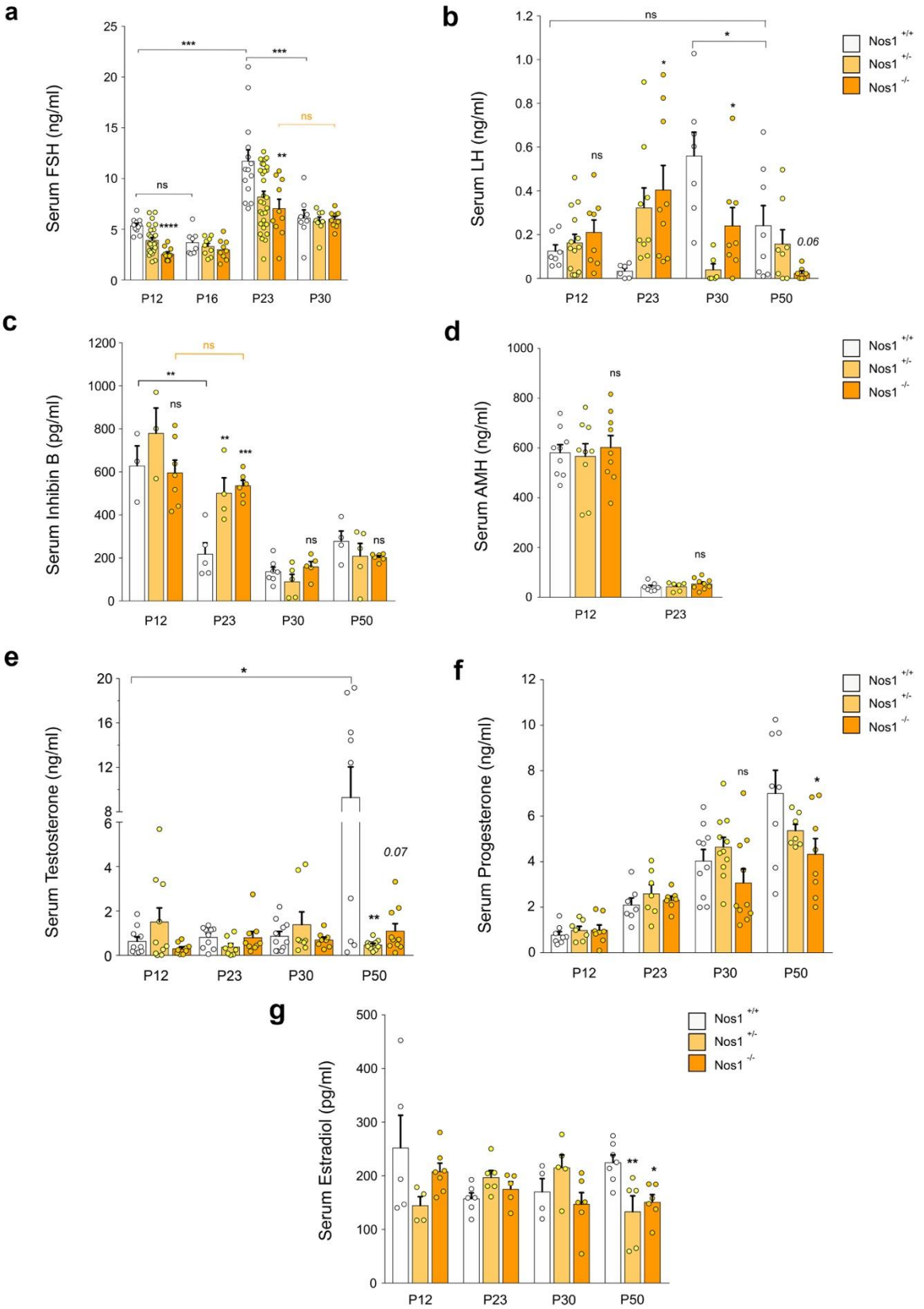

Figure 1. nNOS activity shapes the pattern of minipuberty in male mice and alters the pubertal profile of circulating sex hormones. (a-g) Circulating levels of (a) FSH, (b) LH, (c) inhibin B, (d) AMH, (e) testosterone, (f) progesterone and (g) estradiol in male Nos1+/+, Nos1+/- and Nos1-/- mice during different postnatal stages of development. Hormonal values in Nos1+/+ mice are compared with those of Nos1+/- and Nos1-/- mice for

each group of measurements (one-way ANOVA with Tukey's post-hoc test for a-d, f-g and Kruskal-Wallis with Dunn's post-hoc test for e). When applicable, comparisons between two developmental stages of the same genotype are indicated in the graph (unpaired t-test for a-d, f-g and Mann-Whitney U test for e). * $P < 0.05$; ** $P < 0.01$; *** $P < 0.001$. Values indicate means ± SEM. N=3-8 independent litters.

nNOS activity increases during minipuberty in the male hypothalamus

The infantile period has been recognized as key for the establishment of a mature GnRH neural network, including the activation of nNOS neurons in the OV/MePO in female mice (Messina et al., 2016; Chachlaki et al., 2017a; Pellegrino et al., 2021; Chachlaki et al., 2022). In order to study this preoptic nNOS neuronal population in males during sexual maturation, we measured immunoreactivity for nNOS as well as phosphorylation-activated nNOS (P-nNOS), used as a surrogate marker of nNOS activity (Rameau et al., 2007; Parkash et al., 2010), in the male OV during several developmental stages: neonatal (P7), infantile (P12), juvenile (P23, P30), peripubertal (P50) and adult (P90). Our results show that nNOS immunoreactivity was already present in the OV/MePO by the neonatal period, and nNOS mRNA and protein expression not change substantially during postnatal development (Fig. 2a-b, S1, 4). Phosphorylation of the nNOS protein in the male mouse hypothalamus was negligible during the neonatal period (Fig. 2a-b). However, the proportion of nNOS neurons that were phosphorylated increased significantly at P23 (Fig. 2a-b), simultaneously with the activation of infantile FSH secretion (Fig. 1a), and stayed high until the peripubertal period (P50) (Fig. 2a-b, S1). Intriguingly, P-nNOS immunoreactivity then decreased, reaching infantile values in the OV/MePO of adult male mice (Fig. 2a-b, S1).

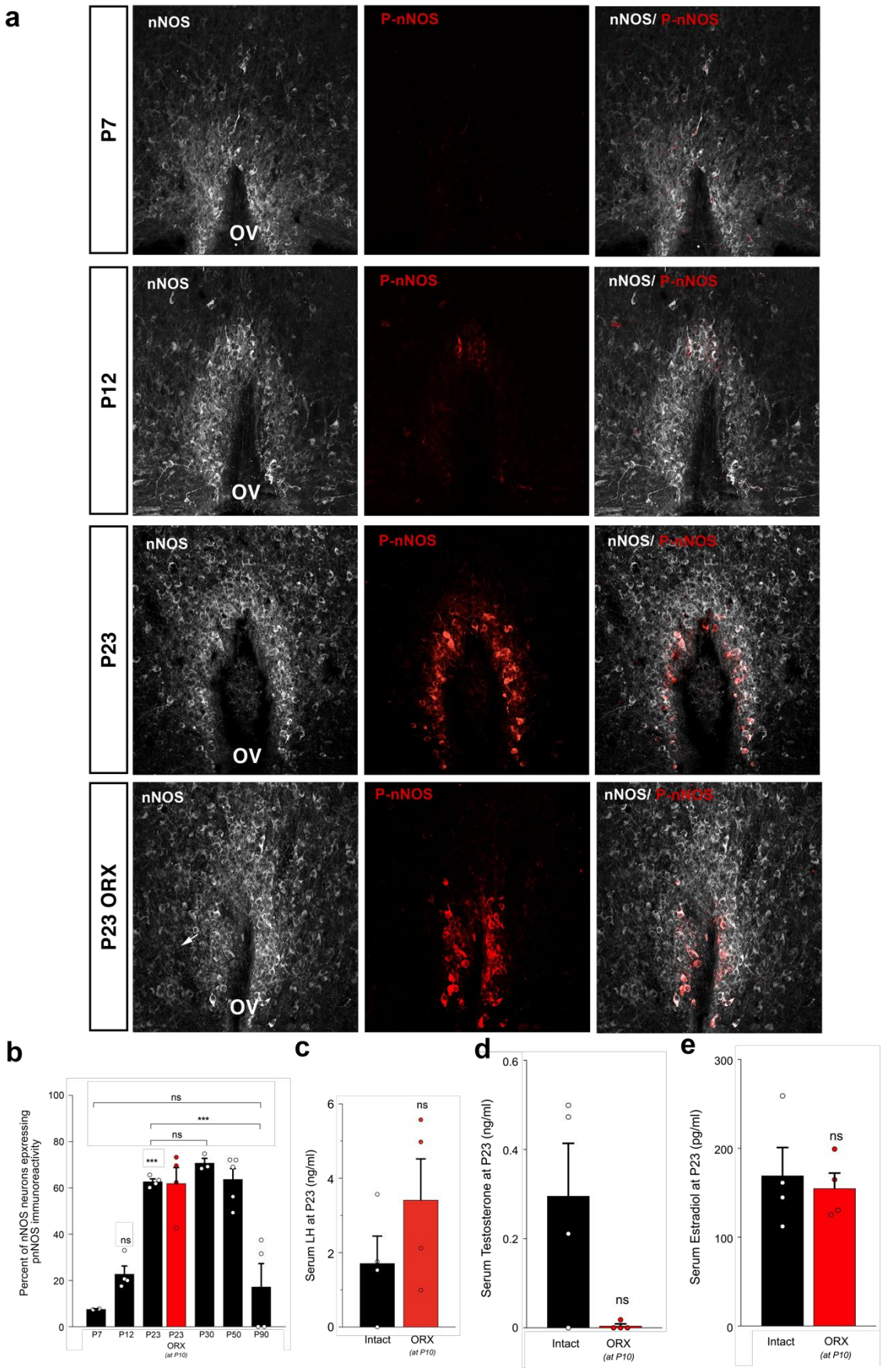

Figure 2. The phosphorylation of nNOS coincides with minipuberty in male mice and is independent of infantile gonadal steroids. (a) nNOS (white) and P-nNOS (red) immunoreactivity in forebrain coronal sections

at the level of the organum vasculosum of the lamina terminalis (OV) in intact male mice at postnatal days 7 and 12 and in intact and orchidectomized (ORX; carried out on P10) mice at P23. (b) Bar graphs illustrate the percentage of nNOS-immunoreactive neurons positive for P-nNOS during postnatal development (P7,12, 23, 30, 50, 90) in the OV in intact male mice and at P23 in ORX mice. P-nNOS levels are compared across all developmental stages (one-way ANOVA with Tukey's post-hoc test). Values after ORX are independently compared to P23 values (unpaired t-test). Asterisks indicate comparisons to P7 P-nNOS levels unless otherwise indicated by a bar. * $P < 0.05$; ** $P < 0.01$; *** $P < 0.001$. Values indicate means ± SEM. N>3 independent litters. (c) Serum LH, (d) testosterone and (e) estradiol levels at P23 in intact and ORX male mice. Values after ORX are independently compared to P23 values in intact male mice (unpaired t-test for c, e and Mann-Whitney U test for d). Values indicate means ± SEM. N>3 independent litters.

nNOS is key for the timely activation of the HPG axis at minipuberty

In female mice, nNOS deficiency is associated with exacerbated minipuberty, with significantly higher LH and FSH values at P12 (Chachlaki et al., 2022). We thus examined the same parameters in male nNOS knockout mice. Gonadotropin measurements in infantile nNOS-deficient male mice revealed that while the FSH levels were decreased at P23 when compared to wild-type littermates (Fig. 1a), LH levels showed a precocious peak at P23 (Fig. 1b). Interestingly, the decreased FSH levels in nNOS knockout mice at P23 were accompanied by an induction of *Fshb* transcripts in the pituitary (Suppl Fig.2). At the same time, circulating inhibin B increased (Fig. 1c) while AMH levels remained unchanged (Fig. 1d), supporting an inhibin B-mediated repression of the release of FSH by gonadotrophs during minipuberty in mutant males (Fig. 1a,c), similar to that seen in females (Chachlaki et al., 2022). In contrast, pituitary *Lhb* and *Gnrhr* mRNA levels were unchanged in mutant mice (Suppl Fig.2). The altered FSH release at the peak of minipuberty in mutant mice was not accompanied by any change in transcriptional profile (Suppl Fig. 3a, b) or testicular histology (Suppl Fig. 3c), and did not translate into any alteration in circulating testosterone, estradiol or progesterone levels during infantile development (Fig. 1e-g). However, peripubertal (P50) LH levels in male mutants were lower than in their wild-type littermates (Fig. 1b), and associated with lower serum estradiol and progesterone levels, at a time when wild-type levels of the latter show a tendency to increase (Fig. 1f, g). Examination of circulating testosterone levels revealed a delay in the postnatal increase of testosterone; nNOS-deficient mice showed lower testosterone levels at P50 than wild-type mice ($p=0.07$) (Fig. 1e). Together with the delay in other maturational processes such as balanopreputial separation (Chachlaki et al., 2022), these results suggest a shift in the gonadotropin-gonadal-steroid profile in the absence of nNOS activity in male mice during postnatal development.

Minipubertal nNOS activity in males is influenced by extragonadal estrogens acting through ERα

In females, the phosphorylation and activation of nNOS in the OV/MePO appears to be mediated by the action of estrogens following the minipubertal activation of the ovaries (Chachlaki et al., 2022). To verify if gonadal activity at minipuberty also plays a role in preoptic nNOS activation in males, we examined the expression of AR in the OV/MePO of wild-type animals. Surprisingly, immunofluorescence for AR in the OV/MePO was very low or absent during the infantile period and only rose after weaning, during the juvenile period (Fig. 3a, c). Both *Ar* mRNA and protein levels reached a peak during the peripubertal period at P50, but even then, only 10% of nNOS neurons expressed AR (Fig. 3a, c, S4). Equally unexpectedly, when we orchidectomized male wild-type pups at P10 and quantified P-nNOS levels at P23, the already low circulating testosterone flatlined (Fig. 2 d) but both P-nNOS expression at P23 (Fig. 2a, b) and circulating LH levels remained unaffected (Fig. 2c). Altogether, these data disqualify gonadal testosterone production as the main trigger for nNOS activation during early postnatal development.

In stark contrast, >70% of nNOS neurons in the OV/MePO expressed ERα throughout postnatal development, starting as early as P12 (Fig. 3b, d), as in females (Chachlaki et al., 2017b). Orchidectomy at P10 had no effect on circulating estrogens at P23 in male mice, and *Esr1* mRNA expression in the POA did not change during the prepubertal period (Fig. 2e, S4). We therefore tested the possibility that the increase in P-nNOS levels during postnatal development was mediated by ERα by selectively blocking ERα activity between P10 and P23 using the daily intraperitoneal injections of the specific ERα antagonist, MPP dihydrochloride. Intriguingly, although MPP treatment had no effect on circulating estradiol or testosterone levels in infantile mice (Fig. 4c, d), they significantly decreased the percentage of nNOS neurons positive for P-nNOS at P23 (Fig. 4a, b), supporting a previously unsuspected role for extragonadal estrogens in the minipubertal activation of nNOS neurons in males.

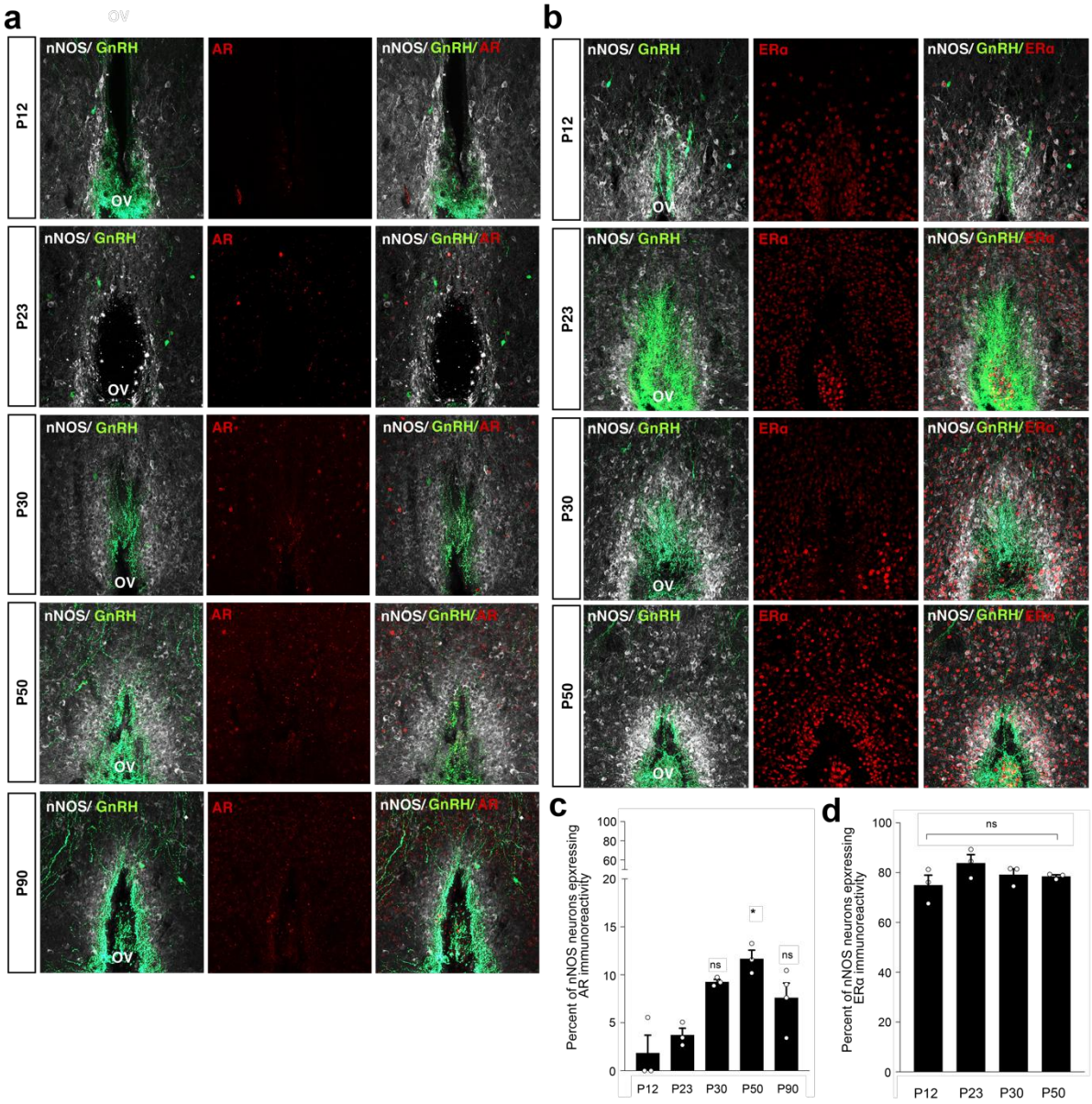

Figure 3. Expression of the androgen receptor and estrogen receptor alpha in the OV/MePO of male mice during postnatal development. (a-b) Immunolabeling at the level of the organum vasculosum of the lamina terminalis (OV) of cells expressing nNOS (white), GnRH (green) and (a) androgen receptor (AR; red) or (b) estrogen receptor alpha (ERα) in intact male mice at different stages of postnatal development. (c-d) Bar graphs illustrate the percentage of nNOS-immunoreactive neurons also expressing AR or ERα during postnatal development in the OV in intact male mice. nNOS/AR or nNOS/ERα co-expression levels are compared across all developmental stages (Kruskal-Wallis with Dunn's post-hoc test). Values are compared to P12 levels. * $P<0.05$. Values indicate means ± SEM. N>3 independent litters.

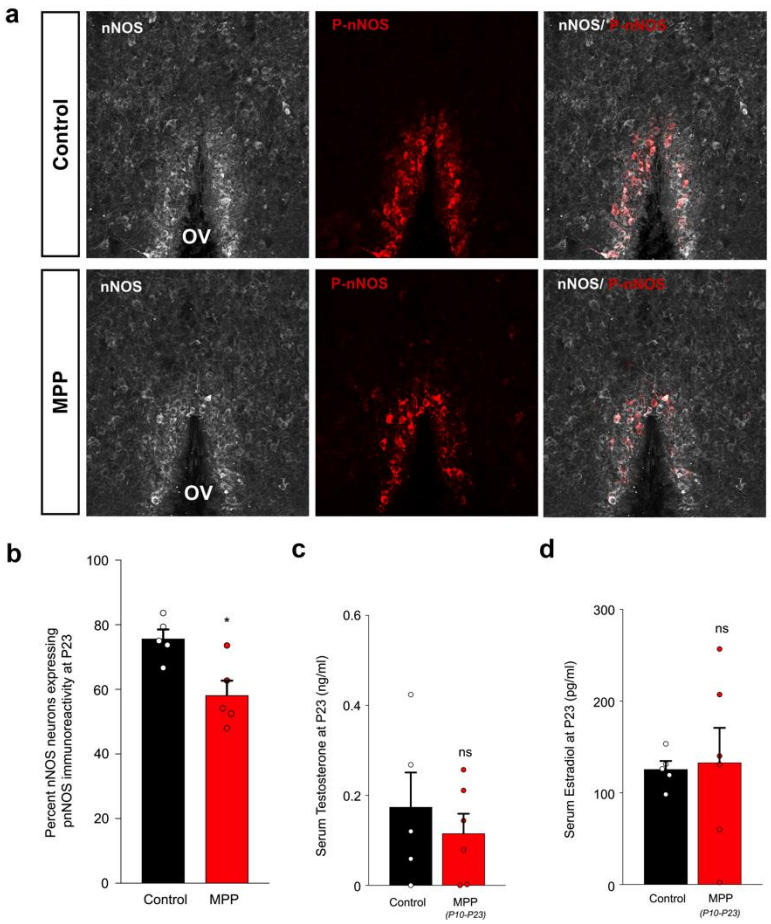

Figure 4. Effect of the ERα antagonist MPP on nNOS phosphorylation and circulating levels of sex hormones in infantile male mice. (a) Immunolabeling for nNOS (white) and P-nNOS (red) at the level of the organum vasculosum of the lamina terminalis (OV) of male mice having received MPP dihydrochloride (an ERα-specific antagonist) or vehicle daily between P10 and P23. (b) Bar graphs illustrate the percentage of nNOS-immunoreactive neurons positive for P-nNOS at P23 in the OV in control (vehicle-treated) or MPP-treated (P10-P23) male mice. Values after MPP treatment from P10 to P23 are compared with P23 values in control male mice (unpaired t-test). * $P<0.05$. Values indicate means ± SEM. N>3 independent litters. (c) Serum testosterone and (d) estradiol levels at P23 in mice having received MPP or vehicle daily from P10 to P23. Values after MPP treatment are compared to P23 values in control (vehicle-treated) male mice (unpaired t-test). Values indicate means ± SEM. N>3 independent litters.

Discussion

The role of nNOS activity, and subsequent NO release, in the regulation of the neuroendocrine axis has received increasing attention in recent years (Bellefontaine et al., 2011; Chachlaki et al., 2017b, 2017a; Delli et al., 2021; Silva et al., 2022; Chachlaki et al., 2022). Recent findings linking nNOS loss-of-function mutations with congenital hypogonadotropic hypogonadism (CHH) due to GnRH deficiency in human patients (Chachlaki et al., 2022) have substantiated the

infertility observed in nNOS knockout mouse models (Huang et al., 1993; Gyurko et al., 2002; Hanchate et al., 2012; Chachlaki et al., 2022). However, very little is known about how NO controls the first postnatal activation of the GnRH system, i.e. minipuberty, a period considered key for the establishment of adult reproductive physiology.

Human studies have already identified important sex differences in the appearance of minipuberty (Kuiri-Hänninen et al., 2011a, 2011b), suggesting that distinct mechanisms could control the postnatal maturation of the HPG axis in the two sexes. In mice, minipuberty has not been extensively studied. In female mice, minipuberty, as defined by a surge in FSH production, begins at around P12 and terminates by the beginning of the juvenile period (around P23) (Prevot et al., 2003; François et al., 2017; Chachlaki et al., 2022). In males, the occurrence of balanopreputial separation, an external sign of sexual maturation, is often confused with the onset of puberty, defined by the ability to reproduce, i.e. the appearance of motile sperm along with high circulating testosterone levels, which only occurs around P55, (Prevot, 2015). Hence, even though minipuberty is shifted in males, reaching a high point at around P23, corresponding to the transition between the infantile and juvenile periods marked by weaning, and terminating at the end of the juvenile stage (around P30), in both male and female mice, minipuberty is an event that is temporally quite distinct from pubertal onset, occurring almost a month earlier. This time window is also in accordance with the gradual increase in GnRH episodic release occurring at the end of the infantile period and reaching zenith values during the juvenile stage, corresponding to male minipuberty, a result that has been also demonstrated in rats (Bourguignon and Franchimont, 1984). As prior reports have also highlighted (Sharpe et al., 1999), FSH concentrations are inversely correlated with inhibin B levels/AMH throughout postnatal development, suggesting that in males, the negative feedback exerted by infantile inhibin B levels controls the timing of minipuberty.

Male minipubertal changes are also staggered, with LH levels increasing around the end of the juvenile period (P30), concomitantly with the end of the FSH surge, and dropping back to infantile values during the peripubertal period at P50, in parallel to *Gnrh* mRNA levels. This minipubertal FSH/LH profile may reflect a primary role for FSH, which is involved in the maturation of spermatogonia and Sertoli cell function, in the first stages of male HPG axis development, in contrast to the involvement of LH in later stages of spermatogenesis, when it induces intratesticular testosterone production and supports Leydig cell function (O'Shaughnessy, 2015; Smith and Walker, 2015). Indeed, in agreement with early reports (Selmanoff et al., 1977; Jean-Faucher et al., 1978; Pang and Tang, 1984), our results reveal no high infantile testosterone production in males. Interestingly, estradiol levels remained high throughout the developmental stages studied, similar to observations in females (Chachlaki et al., 2022). Although the absolute concentrations we report here match imperfectly with previous reports (François et al., 2017), our finding supports an important role for this so-called "female hormone" in male reproductive development (Cooke et al., 2017) and, in

particular, the postnatal maturation of the hypothalamic GnRH neural network, of which nNOS neurons are an integral part.

GnRH production during minipuberty (similar to the pubertal GnRH surge) exerts a self-priming effect: the GnRH-induced production of gonadotropins is responsible for gonadal maturation, while steroid hormones resulting from this gonadal maturation exert control on the GnRH secretory pattern. nNOS neurons, which express AR and ERα, seem to be well poised to convey the necessary gonadal information to hormonally-blind GnRH cells. In male mice, as in females (Messina et al., 2016; Chachlaki et al., 2022), the activation of OV/MePO nNOS cells increases along with the rise in circulating FSH levels at P23, indicating that it is coupled with minipuberty. Surprisingly though, the OV/MePO region in the male hypothalamus was devoid of AR immunoreactivity until the early juvenile stage (P23). It gradually increased to reach its highest values peripubertally (P50), but only 11.7% of nNOS cells co-expressed AR even at this age. However, the vast majority of nNOS neurons of the OV/MePO expressed ERα as early as P12 both in male and female mice (Chachlaki et al., 2017b), supporting a key role for these neurons in the awakening and priming of the GnRH system at minipuberty. Furthermore, these results suggest that the presence of ERα, but not AR, is important for the integration of hormonal information during the infantile period in both sexes.

Estrogenic signals have been shown to be probable determinants for the activity of nNOS cells in female mice during minipubertal and pubertal as well as postpubertal activation of the GnRH system (d'Anglemont de Tassigny et al., 2009; Parkash et al., 2010; Chachlaki et al., 2022), and the ovariectomy of infantile female mice blunts the minipubertal phosphorylation of nNOS protein (Chachlaki et al, 2022). To our great surprise, however, orchidectomy did not have a similar effect on either nNOS phosphorylation in the OV/MePO or the LH profile of infantile male mice. This is in agreement with prior findings in the rhesus monkey showing that the postnatal functional maturation of the male HPG axis is testis- and male-gonadal-steroid-independent (Plant, 1980). Instead, it could be that, at least in males, an extragonadal source provides the estrogenic input necessary to promote the activation of nNOS and subsequently, the GnRH system. In fact, in males, the testes produce only about 20% of circulating estrogens, with the majority of estrogenic content coming from the conversion of testosterone by aromatase (*Cyp19a1*) in the brain or other peripheral tissues such as the adipose tissue, the bones or the skin (Cooke et al., 2017). Interestingly, *Cyp19a1* levels in the POA do not appear to be altered during the prepubertal period or in the absence of nNOS (Suppl. Fig. 4-5), and could continue to contribute to local or circulating estrogen levels. Instead, antagonizing ERα in male mice during infantile development (P10-P23) using MPP dihydrochloride inhibits the minipubertal phosphorylation of the nNOS protein, supporting the idea that estrogens, acting via the ERα-expressing nNOS neurons, are crucial for the maturation of the GnRH system in both female and male mice.

Mutant male mice displayed lower FSH levels and a precocious increase in LH levels at the peak of minipuberty. In fact, the increased inhibin B levels in nNOS-deficient mice at P23, a time at

which inhibin B (and AMH) were seen to decrease by more than half in wild-type mice, could be preventing the increase of FSH and thus the normal initiation of minipuberty. At P30, male mutants showed decreased LH levels while FSH remained unaltered compared to minipubertal values, whereas in wild-type males, the drop in FSH signifies the end of minipubertal GnRH activation (Kuiri-Hänninen et al., 2011b). Considering the importance of pituitary *Pr* downregulation for the GnRH self-priming effect and the termination of the LH surge in cycling females (Turgeon et al., 1999; Gordon et al., 2015), the minipubertal increase in *Esr1* and *Pr* pituitary transcript levels we observed in nNOS-deficient male mice could be associated with the failure of the GnRH system to terminate minipuberty.

Interestingly, the delayed minipuberty in nNOS-deficient male mice was followed by a peripubertal drop in sex steroid levels (testosterone, estradiol and progesterone), similar to decreased circulating estradiol levels in female nNOS-deficient mice (Chachlaki et al., 2022), presumably because deficient GnRH-induced gonadal maturation impacted the later stages of testicular development, including testosterone production by Leydig cells under the control of LH. This in turn would attenuate the negative feedback exerted by gonadal steroids on the male GnRH system, contributing to the improper termination of minipuberty and later acquisition of fertility, as indicated by delayed balanopreputial separation (an external sign of sexual maturation), hypogonadism and subfertility in adulthood (Gyurko et al., 2002; Chachlaki et al, 2022). Intriguingly, the immaturity of the negative feedback operated by gonadal steroids could explain the exaggerated minipuberty observed in prematurely born girls and boys (Kuiri-Hänninen et al., 2011a, 2011b).

Our previous work identified minipuberty and the subsequent maturation of the HPG axis as determining factors for not only the acquisition of reproductive capacity, but also for the establishment of several functions seemingly unrelated to the neuroendocrine axis, such as olfaction, hearing and even cognition in both sexes (Manfredi-Lozano et al., 2022; Chachlaki et al, 2022) The current study reveals several important sex differences in the timing of minipubertal activation of both the nNOS and GnRH systems, as well as an unprecedented common role for estrogens, including those of extragonadal origin in males, in this process.

References

Bellefontaine N, Hanchate NK, Parkash J, Campagne C, De Seranno S, Clasadonte J, D'Anglemont De Tassigny X, Prevot V (2011) Nitric oxide as key mediator of neuron-to-neuron and endothelia-to-glia communication involved in the neuroendocrine control of reproduction. Neuroendocrinology 93:74–89.

Bourguignon J-P, Franchimont P (1984) Puberty-related increase in episodic LHRH release from rat hypothalamus in vitro. Endocrinology 114:1941–1943 Available at: https://doi.org/10.1210/endo-114-5-1941.

Chachlaki K et al. (2022) NOS1 mutations cause hypogonadotropic hypogonadism with sensory and cognitive deficits that can be reversed in infantile mice. Sci Transl Med 14:eabh2369 Available at: https://doi.org/10.1126/scitranslmed.abh2369.

Chachlaki K, Garthwaite J, Prevot V (2017a) The gentle art of saying NO: how nitric oxide gets

497 things done in the hypothalamus. Nat Rev Endocrinol 13:521–535 Available at:
498 http://dx.doi.org/10.1038/nrendo.2017.69.
499 Chachlaki K, Malone SA, Qualls-Creekmore E, Hrabovszky E, Münzberg H, Giacobini P, Ango F,
500 Prevot V (2017b) Phenotyping of nNOS neurons in the postnatal and adult female mouse
501 hypothalamus. J Comp Neurol 525:3177–3189 Available at:
502 http://doi.wiley.com/10.1002/cne.24257 [Accessed October 1, 2017].
503 Chachlaki K, Prevot V (2020) Nitric oxide signalling in the brain and its control of bodily functions.
504 Br J Pharmacol 177:5437–5458 Available at: https://doi.org/10.1111/bph.14800.
505 Cooke PS, Nanjappa MK, Ko C, Prins GS, Hess RA (2017) Estrogens in Male Physiology. Physiol
506 Rev 97:995–1043 Available at: https://doi.org/10.1152/physrev.00018.2016.
507 d'Anglemont de Tassigny X, Campagne C, Steculorum S, Prevot V (2009) Estradiol induces physical
508 association of neuronal nitric oxide synthase with NMDA receptor and promotes nitric oxide
509 formation via estrogen receptor activation in primary neuronal cultures. J Neurochem 109:214–
510 224 Available at: http://www.ncbi.nlm.nih.gov/pmc/articles/PMC2743827/.
511 Delli V, Silva MSB, Prévot V, Chachlaki K (2021) The KiNG of reproduction: Kisspeptin/ nNOS
512 interactions shaping hypothalamic GnRH release. Mol Cell Endocrinol 532:111302 Available at:
513 https://www.sciencedirect.com/science/article/pii/S0303720721001465.
514 Devillers MM, Petit F, Cluzet V, François CM, Giton F, Garrel G, Cohen-Tannoudji J, Guigon CJ
515 (2019) FSH inhibits AMH to support ovarian estradiol synthesis in infantile mice. J Endocrinol
516 240:215–228 Available at: https://joe.bioscientifica.com/view/journals/joe/240/2/JOE-18-
517 0313.xml.
518 Fonseca H, Powers KS, Gonçalves D, Santos A, M.P. M, Duarte JA (2012) Physical Inactivity is a
519 Major Contributor to Ovariectomy-Induced Sarcopenia. Int J Sports Med 33:268–278.
520 François CM, Petit F, Giton F, Gougeon A, Ravel C, Magre S, Cohen-Tannoudji J, Guigon CJ (2017)
521 A novel action of follicle-stimulating hormone in the ovary promotes estradiol production
522 without inducing excessive follicular growth before puberty. Sci Rep 7:46222 Available at:
523 http://europepmc.org/abstract/MED/28397811.
524 Gordon A, Garrido-Gracia JC, Aguilar R, Sánchez-Criado JE (2015) Understanding the regulation of
525 pituitary progesterone receptor expression and phosphorylation. REPRODUCTION 149:615–
526 623 Available at: https://rep.bioscientifica.com/view/journals/rep/149/6/615.xml.
527 Gyurko R, Leupen S, Huang PL (2002) Deletion of Exon 6 of the Neuronal Nitric Oxide Synthase
528 Gene in Mice Results in Hypogonadism and Infertility. Endocrinology 143:2767–2774
529 Available at:
530 http://www.ncbi.nlm.nih.gov/entrez/query.fcgi?cmd=Retrieve&db=PubMed&dopt=Citation&lis
531 t_uids=12072412.
532 Hanchate NK, Parkash J, Bellefontaine N, Mazur D, Colledge WH, d'Anglemont de Tassigny X,
533 Prevot V (2012) Kisspeptin-GPR54 Signaling in Mouse NO-Synthesizing Neurons Participates
534 in the Hypothalamic Control of Ovulation. J Neurosci 32:932–945.
535 Herbison AE (2015) Chapter 11 - Physiology of the Adult Gonadotropin-Releasing Hormone
536 Neuronal Network. In (Plant TM, Zeleznik AJBT-K and NP of R (Fourth E, eds), pp 399–467.
537 San Diego: Academic Press. Available at:
538 http://www.sciencedirect.com/science/article/pii/B9780123971753000119.
539 Huang PL, Dawson TM, Bredt DS, Snyder SH, Fishman MC (1993) Targeted disruption of the
540 neuronal nitric oxide synthase gene. Cell 75:1273–1286 Available at:
541 http://www.sciencedirect.com/science/article/pii/009286749390615W.
542 Jean-Faucher C, Berger M, de Turckheim M, Veyssiere G, Jean C (1978) Developmental patterns of
543 plasma and testicular testosterone in mice from birth to adulthood. Acta Endocrinol (Copenh)
544 89:780–788 Available at:
545 https://eje.bioscientifica.com/view/journals/eje/89/4/acta_89_4_013.xml.
546 Kuiri-Hänninen T, Kallio S, Seuri R, Tyrväinen E, Liakka A, Tapanainen J, Sankilampi U, Dunkel L
547 (2011a) Postnatal Developmental Changes in the Pituitary-Ovarian Axis in Preterm and Term
548 Infant Girls. J Clin Endocrinol Metab 96:3432–3439 Available at:
549 http://dx.doi.org/10.1210/jc.2011-1502.
550 Kuiri-Hänninen T, Sankilampi U, Dunkel L (2014) Activation of the Hypothalamic-Pituitary-Gonadal
551 Axis in Infancy: Minipuberty. Horm Res Paediatr 82:73–80 Available at:

552 http://www.karger.com/DOI/10.1159/000362414.
553 Kuiri-Hänninen T, Seuri R, Tyrväinen E, Turpeinen U, Hämäläinen E, Stenman U-HU-H, Dunkel L,
554 Sankilampi U, Kuiri-Hänninen T, Seuri R, Tyrväinen E, Turpeinen U, Hämäläinen E, Stenman
555 U-HU-H, Dunkel L, Sankilampi U (2011b) Increased Activity of the Hypothalamic-Pituitary-
556 Testicular Axis in Infancy Results in Increased Androgen Action in Premature Boys. J Clin
557 Endocrinol Metab 96:98–105 Available at: http://dx.doi.org/10.1210/jc.2010-1359.
558 Lein ES et al. (2007) Genome-wide atlas of gene expression in the adult mouse brain. Nature
559 445:168–176 Available at: http://dx.doi.org/10.1038/nature05453.
560 Manfredi-Lozano M et al. (2022) GnRH replacement rescues cognition in Down syndrome. Science
561 (80-) 377:eabq4515 Available at: https://doi.org/10.1126/science.abq4515.
562 Messina A, Langlet F, Chachlaki K, Roa J, Rasika S, Jouy N, Gallet S, Gaytan F, Parkash J, Tena-
563 Sempere M, Giacobini P, Prevot V (2016) A microRNA switch regulates the rise in
564 hypothalamic GnRH production before puberty. Nat Neurosci 19:835–844 Available at:
565 http://dx.doi.org/10.1038/nn.4298.
566 Moenter SM (2017) GnRH Neurons on LSD: A Year of Rejecting Hypotheses That May Have Made
567 Karl Popper Proud. Endocrinology 159:199–205 Available at: https://doi.org/10.1210/en.2017-
568 03040.
569 O'Shaughnessy P (2015) Chapter 14 - Testicular Development. In (Plant TM, Zeleznik AJBT-K and
570 NP of R (Fourth E, eds), pp 567–594. San Diego: Academic Press. Available at:
571 http://www.sciencedirect.com/science/article/pii/B9780123971753000144.
572 Pang SF, Tang F (1984) Sex differences in the serum concentrations of testosterone in mice and
573 hamsters during their critical periods of neural sexual differentiation. J Endocrinol 100:7–11
574 Available at: https://joe.bioscientifica.com/view/journals/joe/100/1/joe_100_1_002.xml.
575 Parkash J, D'Anglemont De Tassigny X, Bellefontaine N, Campagne C, Mazure D, Buée-Scherrer V,
576 Prevot V (2010) Phosphorylation of N-methyl-D-aspartic acid receptor-associated neuronal
577 nitric oxide synthase depends on estrogens and modulates hypothalamic nitric oxide production
578 during the ovarian cycle. Endocrinology 151:2723–2735.
579 Plant TM (1980) The Effects of Neonatal Orchidectomy on the Developmental Pattern of
580 Gonadotropin Secretion in the Male Rhesus Monkey (Macaca mulatta)*. Endocrinology
581 106:1451–1454 Available at: https://doi.org/10.1210/endo-106-5-1451.
582 Prevot V (2015) Chapter 30 - Puberty in Mice and Rats. In: Knobil and Neill's Physiology of
583 Reproduction, 4th ed. (Plant TM, Zeleznik AJBT-K and NP of R (Fourth E, eds), pp 1395–1439.
584 San Diego: Academic Press. Available at:
585 http://www.sciencedirect.com/science/article/pii/B9780123971753000302.
586 Prevot V, Rio C, Cho GJ, Lomniczi A, Heger S, Neville CM, Rosenthal NA, Ojeda SR, Corfas G
587 (2003) Normal Female Sexual Development Requires Neuregulin–erbB Receptor Signaling in
588 Hypothalamic Astrocytes. J Neurosci 23:230 LP – 239 Available at:
589 http://www.jneurosci.org/content/23/1/230.abstract.
590 Rameau GA, Tukey DS, Garcin-Hosfield ED, Titcombe RF, Misra C, Khatri L, Getzoff ED, Ziff EB
591 (2007) Biphasic Coupling of Neuronal Nitric Oxide Synthase Phosphorylation to the NMDA
592 Receptor Regulates AMPA Receptor Trafficking and Neuronal Cell Death. J Neurosci
593 27:3445–3455 Available at: http://www.jneurosci.org/content/27/13/3445.abstract.
594 Selmanoff MK, Goldman BD, Ginsburg BE (1977) Developmental Changes in Serum Luteinizing
595 Hormone, Follicle Stimulating Hormone and Androgen Levels in Males of Two Inbred Mouse
596 Strains1. Endocrinology 100:122–127 Available at: https://doi.org/10.1210/endo-100-1-122.
597 Sharpe R, Turner K, McKinnell C, Groome NP, Atanassova N, Millar MR, Buchanan DL, Cooke
598 ANDPS (1999) Inhibin B Levels in Plasma of the Male Rat from Birth to Adulthood: Effect of
599 Experimental Manipulation of Sertoli Cell Number. J Androl 20:94–101 Available at:
600 https://doi.org/10.1002/j.1939-4640.1999.tb02501.x.
601 Silva MSB, Decoster L, Trova S, Mimouni NEH, Delli V, Chachlaki K, Yu Q, Boehm U, Prevot V,
602 Giacobini P (2022) Female sexual behavior is disrupted in a preclinical mouse model of PCOS
603 via an attenuated hypothalamic nitric oxide pathway. Proc Natl Acad Sci 119:e2203503119
604 Available at: https://doi.org/10.1073/pnas.2203503119.
605 Smith LB, Walker WH (2015) Chapter 16 - Hormone Signaling in the Testis. In (Plant TM, Zeleznik
606 AJBT-K and NP of R (Fourth E, eds), pp 637–690. San Diego: Academic Press. Available at:

http://www.sciencedirect.com/science/article/pii/B9780123971753000168.
Steyn FJ, Wan Y, Clarkson J, Veldhuis JD, Herbison AE, Chen C (2013) Development of a Methodology for and Assessment of Pulsatile Luteinizing Hormone Secretion in Juvenile and Adult Male Mice. Endocrinology 154:4939–4945 Available at: http://dx.doi.org/10.1210/en.2013-1502.
Turgeon JL, Van Patten SM, Shyamala G, Waring DW (1999) Steroid Regulation of Progesterone Receptor Expression in Cultured Rat Gonadotropes*. Endocrinology 140:2318–2325 Available at: https://doi.org/10.1210/endo.140.5.6709.

Acknowledgments

This work has been supported by the European Union Horizon 2020 research and innovation program No 847941 miniNO (to K.C. and V.P.), the European Research Council COST action BM1105 for the study of GnRH deficiency (to V.P.), the Fondation pour la Recherche Médicale (Equipe FRM, DEQ20130326524 to V.P and SPE201803005208 to K.C.), the Agence Nationale de la Recherche (ANR-17-CE16-0015 to V.P.) and the University of Lille (PhD fellowship to V.D.). The authors thank Meryem Tardivel (imaging core facility, BiCeL), Julien Devassine (animal house), Brenda Lammens, Solène Audry, Marie-Hélène Gevaert (Histology, BiCeL) of the PLBS UMS2014-US4, and Amandine Legrand for her expert technical assistance. Graphical abstract was created with BioRender.com.

Supplementary Figures

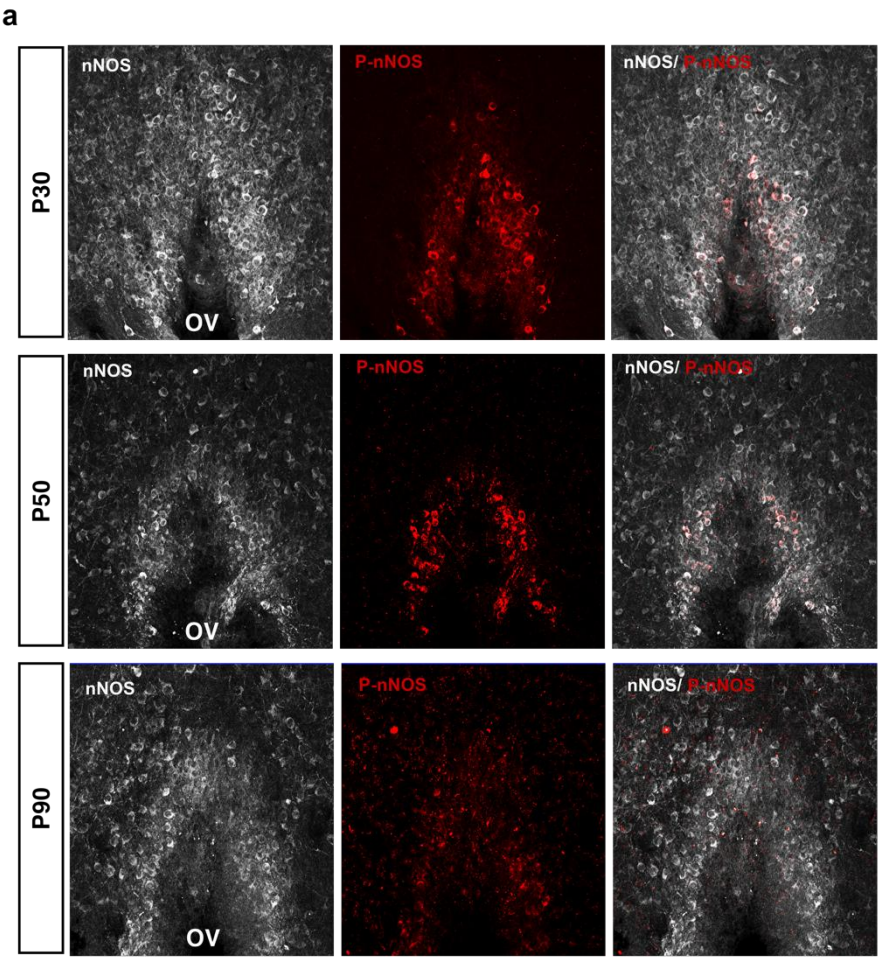

Supplementary Figure 1. Phosphorylation of nNOS in post-minipubertal male mice. nNOS (white) and P-nNOS (red) immunoreactivity in forebrain coronal sections at the level of the organum vasculosum of the lamina terminalis (OV) in intact male mice on postnatal days 30, 50 and 90.

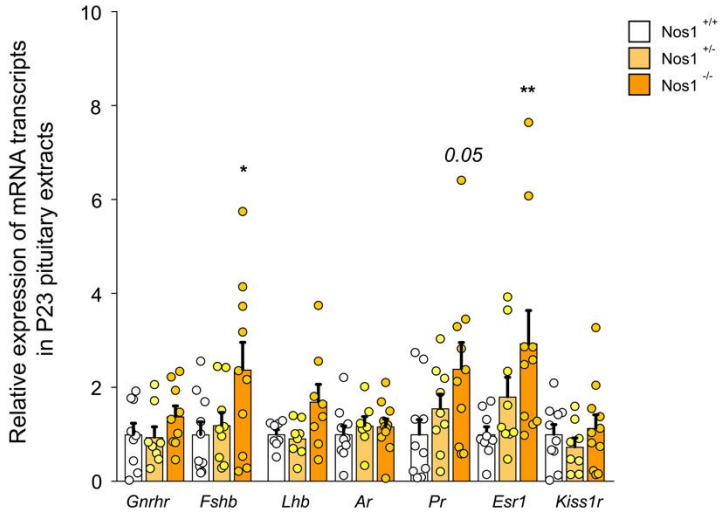

Supplementary Figure 2. nNOS deficiency does not alter minipubertal *Gnrhr* expression but affects the transcriptional profile of steroidogenesis-related genes in the male pituitary. *Gnrhr*, *FSHb*, *LHb*, *Ar*, *Pr*, *Esr1* and *Kiss1r* transcript expression in the pituitary at P23 in wild-type and nNOS-deficient male mice. mRNA expression levels were compared to wild-type values (one-way ANOVA with Tukey's post-hoc test for *Gnrhr*, *FSHb*, *LHb*, *Ar* and *Kiss1r* and Kruskal-Wallis with Dunn's post-hoc test for *Pr* and *Esr1*). * $P < 0.05$; ** $P < 0.01$; Values indicate means ± SEM. N>3 independent litters.

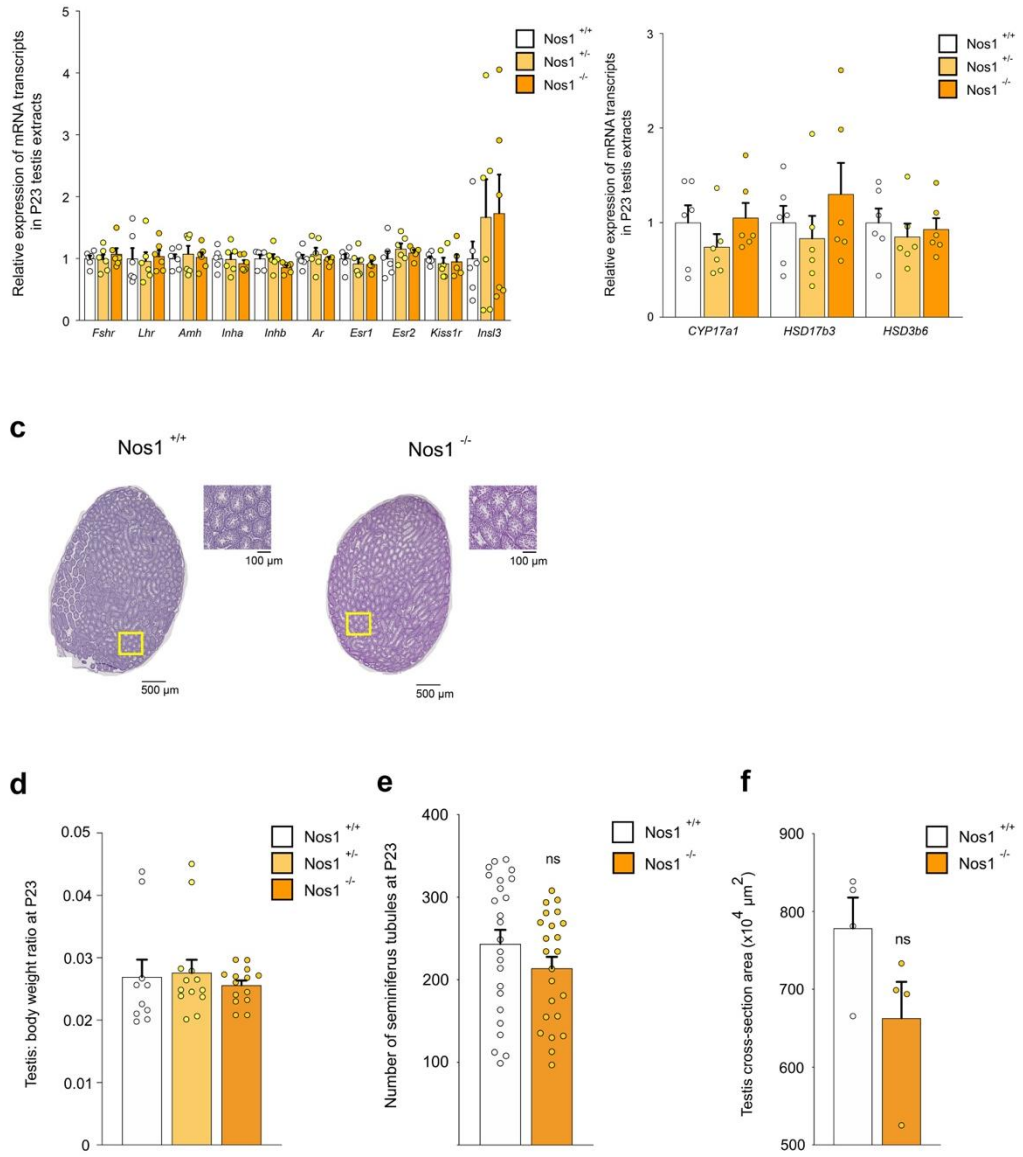

Supplementary Figure 3. nNOS deficiency does not alter minipubertal transcriptional profile of steroidogenic genes or basic morphometric parameters in the testis. (a) *Fshr*, *Lhr*, *Amh*, *Inha*, *Inhb*, *Ar*, *Esr1*, *Esr2*, *Kiss1r* and *Insl3* and (b) *Cyp17a1*, *Hsd17b3* and *Hsd3b6* transcripts expression in the testis at P23 in wild-type and nNOS-deficient mice. (c) Representative images of hematoxylin-eosin-stained testis cross sections from P23 wild-type and nNOS-deficient mice. Scale bar: 500 µm. Square insets indicate magnification, scale bar: 100µm. (d) Testis-to-body weight ratio, (e) total seminiferous tubule count and (f) Cross sectional area of the testis in P23 wild-type and nNOS-deficient male mice. Values are compared to wildtype P23 values (unpaired t-test). Values indicate means ± SEM. N>3 independent litters.

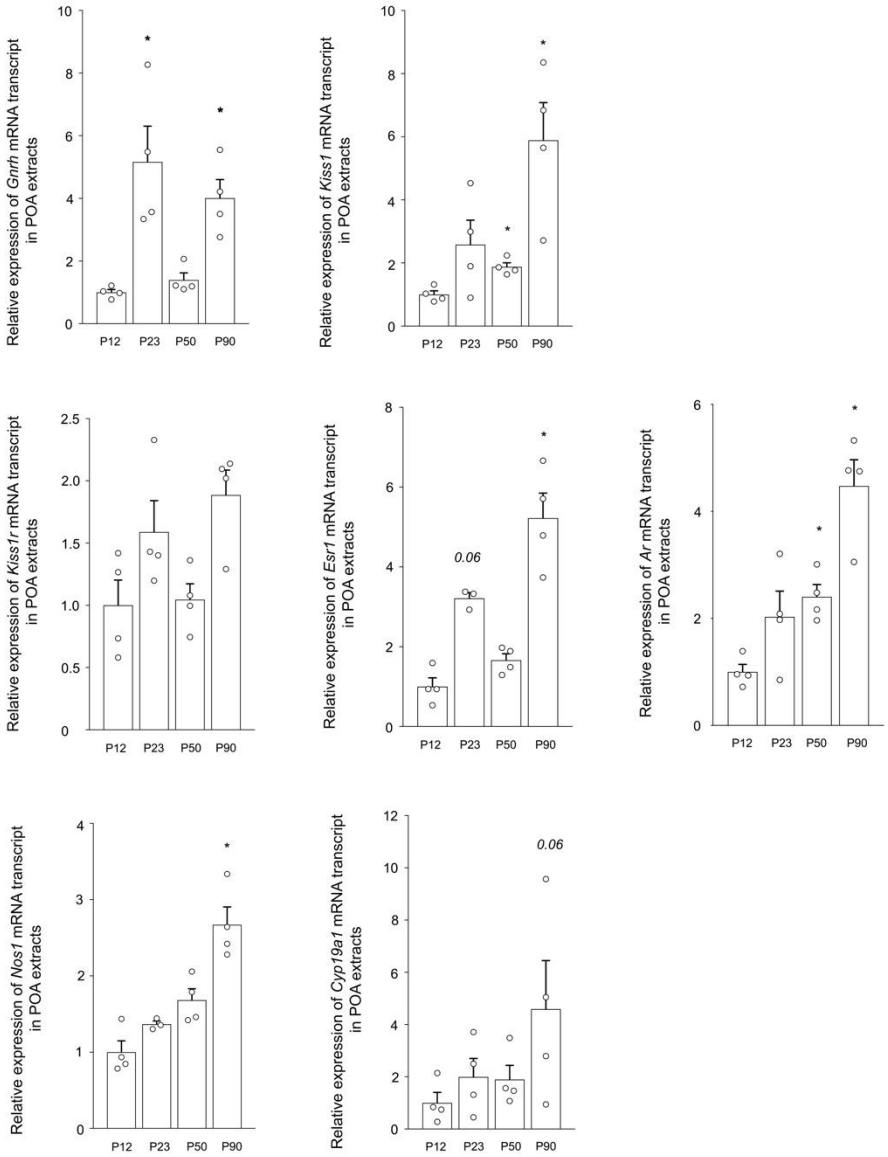

659

660 **Supplementary Figure 4 Minipuberty is not accompanied by changes in the mRNA profile of kisspeptin**
661 **or sex steroid receptors.** *Gnrh*, *Kiss1*, *Kiss1r*, *Esr1*, *Ar*, *Nos1* and *Cyp19a1* transcript expression in the preoptic
662 area at P12, P23, P50 and P90 in wild-type mice. mRNA expression levels were compared to P12 values for
663 each timepoint (Mann-Whitney U test). * $P < 0.05$. Values indicate means ± SEM. N>3 independent litters.

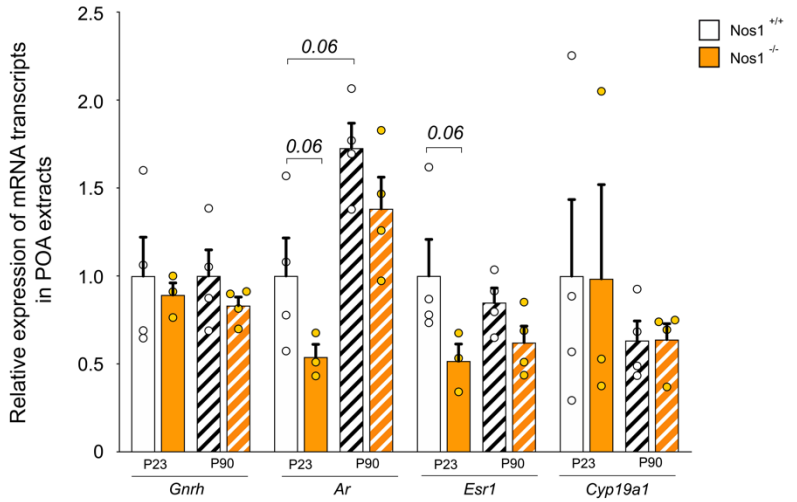

Supplementary Figure 5 nNOS-deficiency does not alter mRNA profile of Gnrh or sex steroid receptors. *Gnrh, Ar, Esr1 and Cyp19a1* transcripts expression in the preoptic area at P23 and P90 in wild-type and nNOS-deficient mice. mRNA expression levels were compared to wildtype values for each timepoint (Mann Whitney). Values indicate means ± SEM. N>3 independent litters.